Regular Article

PHYSICAL CHEMISTRY RESEARCH
Published by the
Iranian Chemical Society
www.physchemres.org
info@physchemres.org

Phys. Chem. Res., Vol. 8, No. 4, 767-787, December 2020

Adsorption of Different Dyes from Aqueous Solutions Using Organo-clay Compposites

Z. Baouch, K.I. Benabadji* and B. Bouras

Laboratory of Organic Electrolytes and Polyelectrolytes Application (LAEPO). Department of Chemistry, Faculty of Sciences, Tlemcen University, B. P. 119 13000 Tlemcen, Algeria

(Received 10 June 2020, Accepted 19 August 2020)

The structural evolution of cost-effective organo-clays; *i.e.*, bentonite modified with various loadings of hexadecyltrimethylammonium bromide (HDTMA-Br), from 50 to 200% of the cationic exchange capacity, labeled as BAS 0.5, BAS 1, BAS 1.2, BAS 1.5 and BAS 2, was investigated. The materials BAS were prepared and then characterized by X-ray diffraction (XRD), infrared spectroscopy (FTIR), and thermal analysis (ATG/DTG). The increase in the basal spacing, from 1.13 to 1.78 nm, was a sufficient confirmation that the surfactant cations were intercalated within the interlayer spaces of bentonite (BA). Batch adsorption experiments were performed to evaluate the adsorption efficiencies of Methylene Blue (MB), Bezathren Red (BzR) and Telon Blue (TB) dyes on the surfactant-modified bentonite from an aqueous solution. Moreover, the effects of several factors, such as the contact time, pH of dye solution, adsorbent dosage, initial dye concentrations, and temperature, on the adsorption capacity were investigated. In addition, the kinetic data were found to follow the pseudo second-order model for the adsorption processes of all three dyes. Afterwards, the equilibrium data were analyzed using the Langmuir and Freundlich isotherm models, and the Langmuir isotherm model turned out to be the most suitable to describe the adsorption of these dyes. It is worth indicating that the calculated Langmuir maximum adsorption capacities increased from 74 to 166.67 mg g^{-1} for Methylene Blue, from zero to 111.1 mg g^{-1} for Bezathren Red, and from zero to 500 mg g^{-1} for Telon Blue. The adsorption process was found to be endothermic in nature, in all cases.

Keywords: Inorganic/organic hybrid materials, Adsorption mechanism, Cationic, Anionic, Vat dyes

INTTRODUCTION

One of the major future challenges facing humanity is to secure the supply of clean water to the world population. It is widely admitted that population growth and pollution have a strong impact on water quality. Indeed, nowadays, dyes utilized in industrial activities are increasingly becoming a problematic class of pollutants to the environment. Due to the complex structure of dyes, their discharge to water bodies engenders bad aesthetic and health consequences [1]. Over the last few years, several classes of dyes have been used in many industrial sectors such as rubber, textiles, cosmetics, plastics, leather, food and paper making [2]. Wastewater discharged from these industries contains a variety of dyes and the majority of them are stable to light, heat and oxidizing agents and are usually non-biodegradable [3], hence the urgent need to remove them from the environment. Dyes can be classified as cationic, anionic, and nonionic (disperse/vat). These three kinds of dyes are the most widely used dyes in many industries. Due to their complex structures, they are not easily biodegradable and can therefore have destructive impacts on the environment [4]. Today, adsorption is viewed as a viable procedure for the removal of dyes from the environment; it is a simple process that is economically feasible and can help to recycle the adsorbents without any harmful residues. Indeed, a large number of studies have investigated the use of various adsorbents intended for the

*Corresponding author. E-mail: bismetdz@yahoo.fr

purpose of reducing dye concentrations in aqueous solutions. Materials like walnut husk [5], modified chitosan composite [6], biochars from crop residues [7], natural zeolite [8], cross-linked succinyl chitosan [9], modified bentonite [10], quaternized poly(4-vinylpyridine) copolymers [11], natural clinoptilolite [12], activated carbon [13], chromium-intercalated montmorillonite [14] and metal oxides [15-18] have been used to remove dyes from aqueous solutions. Clays, such as bentonite, have exhibited high removal efficiency; it was found that their adsorption capacities may exceed that of activated carbon, under the same temperature and pH conditions [19]. The adsorption and desorption of organic molecules on clays depend primarily on the surface properties of these materials and on the chemical properties of their molecules as well [20]. Note that the net negative charge on clays provides them with a high adsorption capacity toward positively charged cations such as cationic dyes, heavy metals, *etc*. However, clays have a poor affinity for negatively charged anionic dyes. It is worth indicating that a simple modification of clays can help to improve their adsorption capacities by the use of cationic polymers or surfactants through straightforward ion-exchange reactions which generate some interactions between the cationic species and the adsorbate [21]. Previous studies have shown that the removal of acid dyes can be better enhanced by the use of modified montmorillonite, in comparison with untreated montmorillonite. It is worth mentioning that modified montmorillonites have previously been prepared and used for Congo red dye adsorption. It was also found that the adsorption efficiency is influenced by the length of alkyl chains present in a series of alkyl ammonium bromides [22]. Several authors have successfully modified montmorillonite using some unconventional modifiers [23], such as gemini surfactants, for the adsorption of organic contaminants [24]. The results obtained showed that the adsorption capacity of surfactant-modified montmorillonites for organic contaminants was greatly improved in comparison with that of natural montmorillonite. The present work aims to investigate the possibility of interposing HDTMA-Br molecules into clay for the purpose of obtaining BAS materials. A BAS is employed as an adsorbent for the removal of three kinds of dyes, namely Methylene Blue (cationic dye), Telon Blue (anionic dye), and Bezathren Red (nonionic dye), from aqueous solutions. Optimization of the adsorption conditions was possible by investigating the influence of different parameters. The equilibrium data obtained were then assessed using various adsorption isotherm models. Some kinetic studies were also conducted in order to evaluate the adsorption mechanism.

EXPERIMENTAL

Materials

The hexadecyltrimethylammonium bromide (HDTMA-Br) was purchased from Sigma Aldrich (99% purity) and used as received. Sodium chloride (NaCl) was provided by Aldrich and used without further purification. Likewise, Methylene Blue (MB), Bezathren Red (BzR) and Telon Blue (TB) were purchased from Sigma-Aldrich and utilized without further purification. Some specific characteristics of these three dyes are summarized in Table 1.

Bentonite Sample

The starting material used in this study was natural bentonite (NB), provided by the National Company of Non-Ferrous Mining Products and Useful Substances (ENOF-Algeria). Natural bentonite, which is essentially composed of montmorillonite (80%), contains a large number of impurities. The chemical composition of natural bentonite (NB) was determined by X-ray fluorescence (XRF) spectrometry, and the data obtained are reported in Table 2.

Raw bentonite was purified under laboratory conditions [25]. In order to remove impurities, such as carbonates, quartz, and organic matter, the bentonite was dispersed in bidistilled water, and the clay fraction (< 2 μm) was recovered through sedimentation. In order to obtain sodium bentonite, the solid phase was then saturated with sodium ions in a 1 M sodium chloride solution and stirred; this operation was repeated three times. When saturation was achieved, the resulting solid was washed with bidistilled water several times in order to remove excess salt; the final product was sodium bentonite (BA). Then, the hexamminecobalt (III) chloride was used to determine the cation exchange capacity (CEC) which was found equal to 85 meq g/100 g.

Table 1. Physicochemical Characteristics of Dyes Used in this Study

Name	Molecular structure	Nature	M_w (g mol^{-1})	λ_{max} (nm)
Methylene Blue (Basic Blue 9)	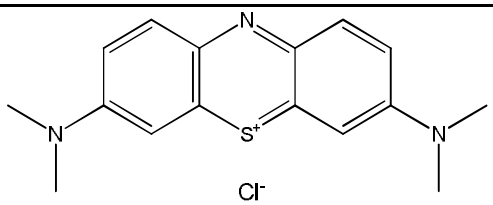	Cationic	319.851	664
Telon Blue (Acid Blue 62)	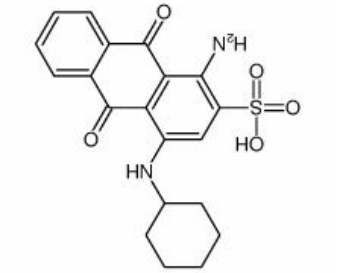	Anionic	400.44	640
Bezathren Red FBB EPS (Disperse 11)	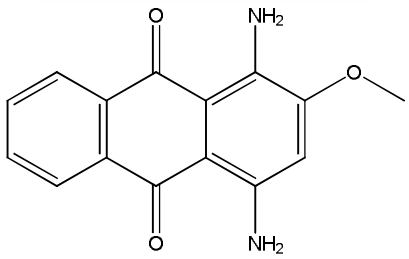	Disperse	268.272	505

Table 2. Chemical Composition of Natural Bentonite

Species	SiO_2	Al_2O_3	Fe_2O_3	CaO	MgO	Na_2O	K_2O	TiO_2	LOI
%(w/w)	65.2	17.25	2.10	1.20	3.10	2.15	0.60	0.20	8.20

Preparation of Organo-clays (BAS)

The amount of 2 g of sodium bentonite (BA) was dispersed into 50 ml of distilled water. Then, 200 ml of the HDTMA-Br solution was added dropwise to this suspension, and the mixture was shaken using a mechanical shaker for 4 h at 80 °C. Note that the initial amounts of HDTMA-Br in the aqueous phase were equivalent to various percentages of CEC (from 50 to 200 meq g/100 g BA). The resulting material was centrifuged at 4000 rpm, for 30 min, to yield a clear supernatant. Afterwards, the solid was washed several times with warm distilled water, until complete disappearance of bromide anions, as indicated by the silver nitrate ($AgNO_3$) test. Next, the ensuing organo-clay was dried at 60 °C, then crushed and

sieved for particles less than 100 μm. The organo-clays obtained were labeled as BAS 0.5, BAS 1, BAS 1.2, BAS 1.5 and BAS 2, according to the percentage of CEC.

Batch Adsorption Studies

The adsorption capacities of the prepared composites for MB, TB and BzR dyes were evaluated using a batch equilibrium procedure. For doing so, the stock dyes solutions (1000 mg l^{-1}) were first prepared by dissolving MB and TB in deionized water. For the vat dye BzR, a sodium hydroxide solution and hydrosulfite salts were used for the preparation of the aqueous solution. The stock solutions were then diluted in deionized water to achieve the desired concentration ranges. Subsequently, the dried sample (25 mg) was immersed in each dye solution (40 ml). The dye solutions containing the adsorbents were then shaken at 400 rpm. Finally, each solution was centrifuged at 4000 rpm for a period of 15 min, and the ensuing supernatant was analyzed using a UV-Vis spectrophotometer (OPTIZEN 1412 UV/VIS) at their maximum wavelengths (664, 495 and 505 nm for MB, TB and BzR, respectively).

Furthermore, adsorption experiments were conducted in conical flasks, at a constant agitation speed of 400 rpm, while varying the pH of the solution from 2 to 11, the adsorbent dosage from 10 to 100 mg, the contact time from 2 to 180 min, the initial dye concentration from 5 to 200 mg l^{-1} and the temperature from 25 to 50 °C.

The adsorption capacity and removal efficiency of the prepared composite were calculated based on the initial and final concentrations of dyes present in the solution, using the following Eq. (1):

$$q_e = \frac{(C_0 - C_e).V}{m} \quad (1)$$

where C_0 and C_e are the initial and equilibrium dye concentrations, respectively, V is the volume of dye aqueous solution (l) and m is the mass of adsorbent (g).

Characterization

The XRD patterns of the samples were obtained with X-ray diffractometer ULTIMA IV (Rigaku, Tokyo, Japan), operating with Copper K_α radiation (λ = 1.54 Å) at 40 kV and 30 mA. All experiments were carried out at ambient temperature with 2θ varying between 2 and 40°, a scan speed of 2°/min and a step size of 0.02°.

Infrared (IR) spectra of the samples were obtained using an Agilent Cary 600 Series FTIR Spectrometer equipped with DRIFT (diffuse reflectance infra-red Fourier transform) spectroscopy. Spectra over the 4,000-400 cm^{-1} range were obtained by the co-addition of 64 scans with a resolution of 4 cm^{-1} and a mirror velocity of 0.6329 cm s^{-1}.

Thermogravimetric analyses of the samples were obtained using High-resolution TGA (TA Instruments Q Series Q600 SDT). 10 mg of finely ground sample was heated in an open platinum crucible with a heating rate of 10 °C min^{-1} and temperature from 50 to 800 °C under a nitrogen atmosphere flow rate of 100 ml min^{-1}.

Determination of pH_{pzc}

The point of zero charge (pH_{pzc}) is the pH for which the net surface charge of the adsorbent is equal to zero. This is an important parameter in determining the adsorption capacity of the surface and the type of surface active centers. In the present work, the pH_{pzc} of the adsorbent (BA and BAS 1.5) was determined using a batch equilibrium method, following the procedures previously outlined by Monvisade *et al*. [26].

RESULTS AND DISCUSSION

X-Ray Diffraction

The X-ray diffraction patterns of the absorbents BA and BAS are presented in Fig. 1a, while the variation of the interlamellar distance (Δd) as a function of the amount of intercalated surfactant molecules is depicted in Fig. 1b.

The interlayer spacing values $d_{(001)}$ of the parent BA and of BAS clay samples were determined using low-angle XRD. For BA, as can be seen in Fig. 1a, a broad peak was observed at 2θ = 7.76° which corresponds to montmorillonite. This result suggests an interlamellar distance $d_{(001)}$ of 11.37 Å. For BAS 0.5 sample (Fig. 1a), corresponding to 0.5 CEC of BA, a sharp peak was observed at 2θ = 6.58°, which corresponds to $d_{(001)}$ = 13.41 Å. Upon the addition of HDTMA molecules, the peak positions shifted to lower angles, in accordance with the HDTMA loading. A displacement of the angle 2θ

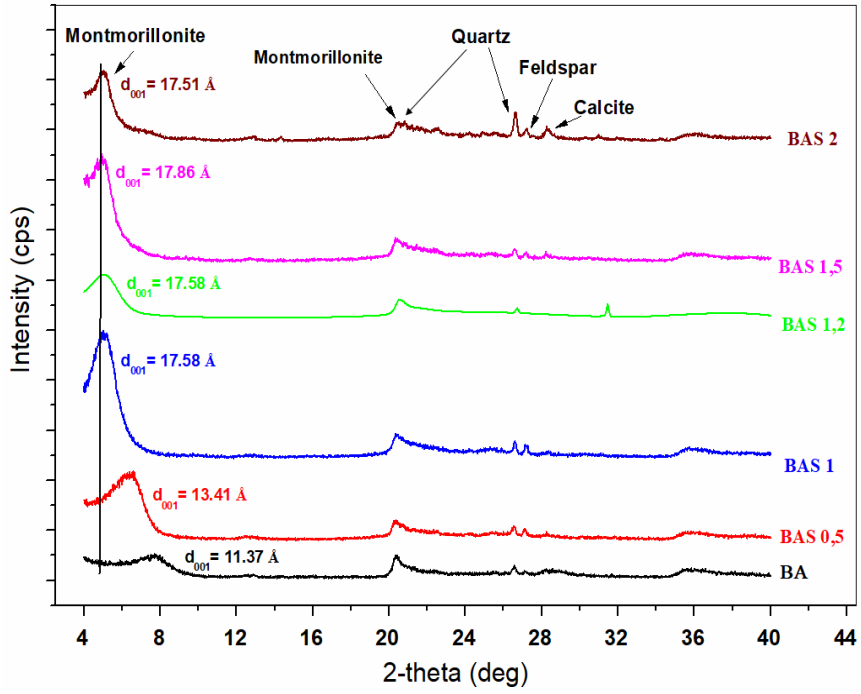

(a)

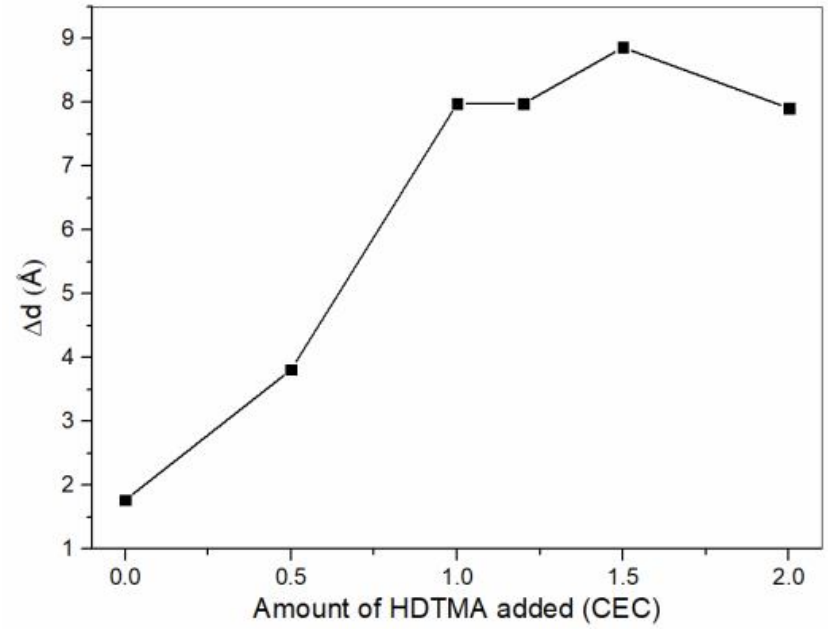

(b)

Fig. 1. XRD analysis of BA and BAS samples and values of their interlamellar distances $d_{(001)}$ at different surfactant concentrations (a) and Δd (b).

was observed from 7.76° to 5.04° with an increase in $d_{(001)}$ values from 11.37 Å for BA to 17.86 Å for the organophilic clay BAS 1.5, confirming the intercalation of ammonium ions in the interlayer space [27]. However, for higher HDTMA loadings, the peak position remained nearly constant, which means that a saturation limit was reached for the intercalation of the HDTMA molecules inside the BA material. These findings are in accordance with the FTIR and TGA results.

A cation exchange process was used to compensate for the excess negative charges, and the sodium ions were replaced by the positively charged surfactant molecules. The thickness of a layer in a single unmodified montmorillonite structural unit was considered to be equal to 9.6 Å [28]. By subtracting the thickness of the single montmorillonite unit (9.6 Å) from the $d_{(001)}$ spacing of the surfactant-modified clay, the interlamellar spacing Δd, occupied by the HDTMA molecules, can be deduced. It is worth noting that the Δd values increased from 3.81 Å in the case of BAS 0.5 to reach 8.26 Å in the case of BAS 1.5; it then remained almost unchanged with greater HDTMA loadings (Fig. 1b).

Infrared Spectroscopy

The IR spectra of BA and BAS, depicted in Fig. 2a, indicate that modification of clay was successfully achieved. It should be noted that the FTIR spectra were characterized by an important absorption band reduction, between 3300 and 3750 cm^{-1}, indicating the new hydrophobic behavior of the BAS samples. The bands corresponding to hydroxyl groups indicated the progressive replacement of water molecules by those of the cationic surfactant [29].

The presence of cationic surfactant molecules in BAS composites was confirmed by the appearance of new absorption bands. The spectra (Fig. 2a) showed additional absorption bands, at 2927 cm^{-1} and 2854 cm^{-1}, which are assigned to the asymmetric and symmetric stretching vibrations of $-CH_2$ groups, respectively.

Another new band appeared at 1464 cm^{-1} was attributed to the bending vibrations of methyl group C-H in the ammonium groups.

When the surfactant loadings were increased, the peak intensity and peak area of the absorption bands at 2927 cm^{-1} and 2854 cm^{-1} for BAS samples became stronger and sharper, exhibiting a sudden initial increase in the incorporation of HDTMA molecules. By increasing the amount of HDTMA loading, these bands shifted towards lower frequencies (Fig. 2b), suggesting a transition from a disordered liquid-like conformation of alkyl chains at low HDTMA loadings to a more ordered state at higher loadings where the modifier alkyl chains exhibited highly ordered all-trans conformations [30].

Thermogravimetric Analysis

In order to investigate the structural properties of modified clays and to estimate the surfactant adsorbed onto sodium bentonite, some thermogravimetric analysis (TGA) experiments were conducted under a nitrogen atmosphere. The TGA and DTG results obtained, presented in Fig. 3a and 3b, indicate that unmodified sodium bentonite (BA) exhibited a mass loss of 5.31% at 64 °C, corresponding to the loss of the interlayer water. A second mass loss of 5.26%, between 170 °C and 800 °C, was related to the dehydration of the BA layers, including condensation of both the intralamellar Al(OH) and structural Al(OH) in clay [31]. The TGA and DTG data of all BAS samples showed a similar degradation profile (Fig. 3a), indicating the presence of both surface bound and intercalated organic modifiers. However, for BAS 0.5 sample, only one peak at around 407 °C was observed, suggesting that at low modifier loadings, intercalation occurs only within the BA interlayers. For BAS samples, the resulting thermograms suggested the occurrence of additional weight losses within the temperature range between 170 and 460 °C. The corresponding degradations could not be observed in the thermogram of the BA sample. These findings indicate that the surfactant molecules adsorbed onto the external surface of the BA sample and intercalated in the interlayer spaces helped to improve the thermal stability of the corresponding composites [32]. Note also that the DTG curves of surfactant-modified sodium bentonite samples (BAS 0.5, BAS 1, BAS 1.2, BAS 1.5 and BAS 2) presented four kinds of weight losses (Table 3). The first one was assigned to the vaporization of free water. It is worth indicating that when the HDTMA loading goes up, these weight losses get smaller. Moreover, the presence of Alkylammonium leads to the conversion of hydrophilic surfaces to hydrophobic

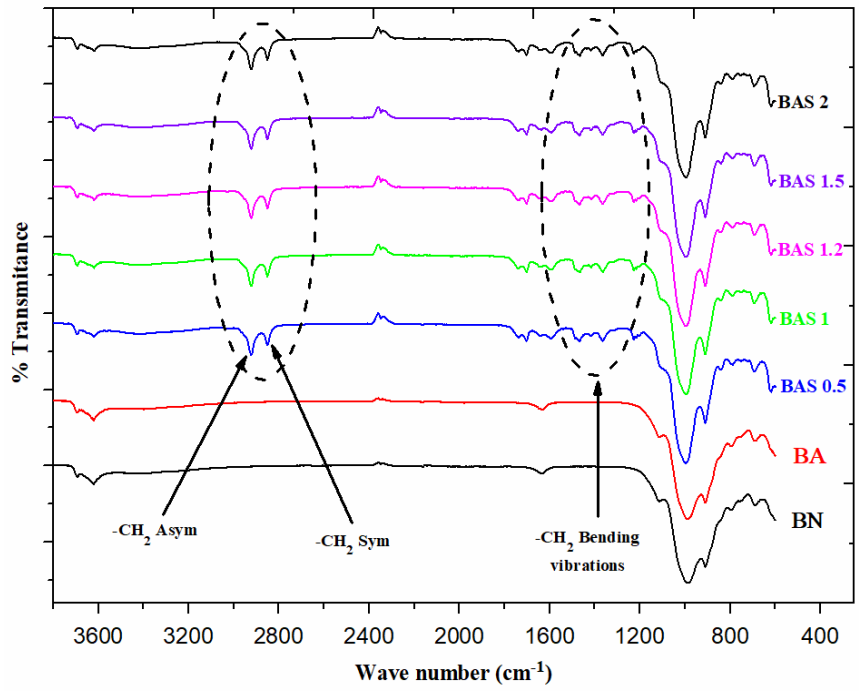

(a)

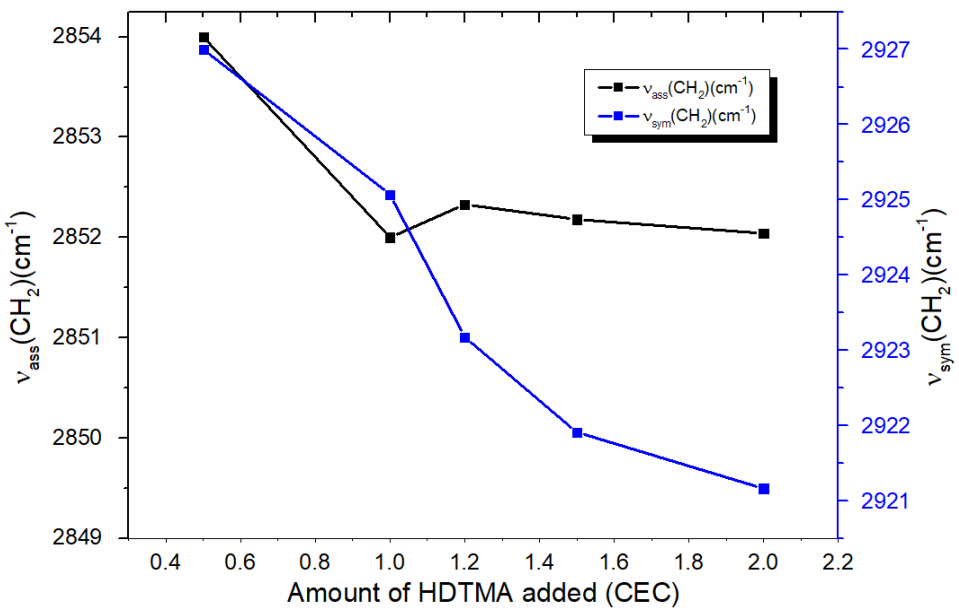

(b)

Fig. 2. (a) IR spectra of BN, BA and BAS samples. (b) Variation of vas(-CH_2-) and vs. (-CH_2-) as a function of HDTMA loading.

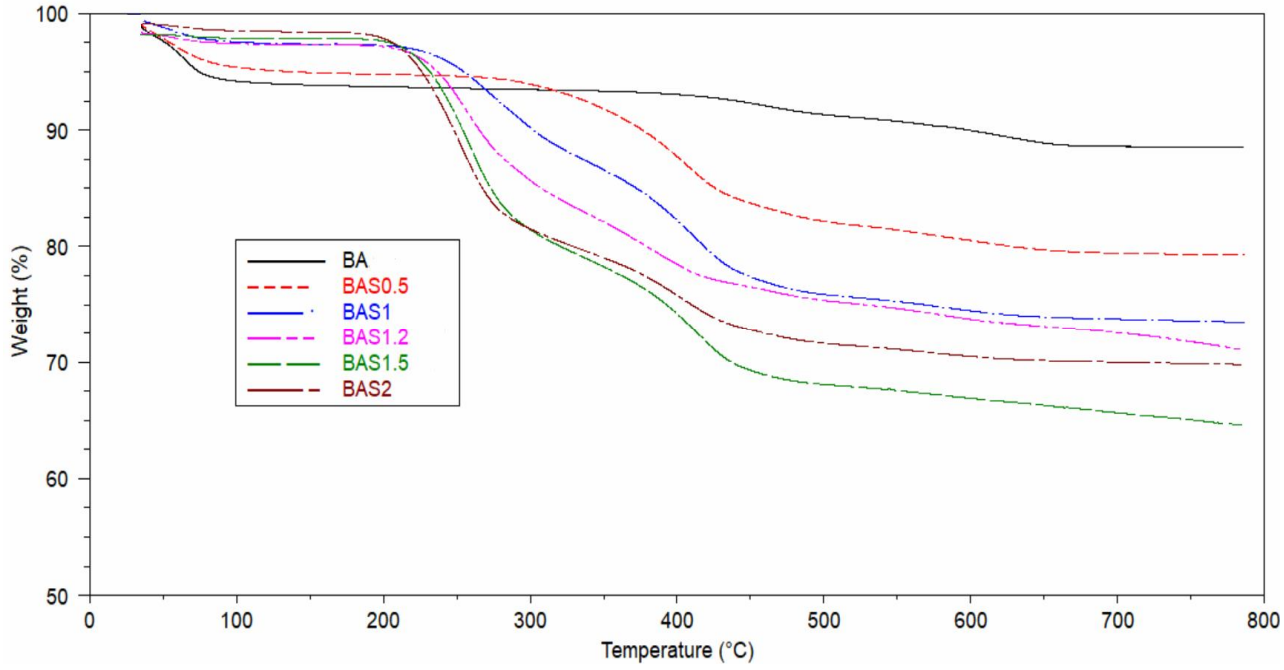

(a)

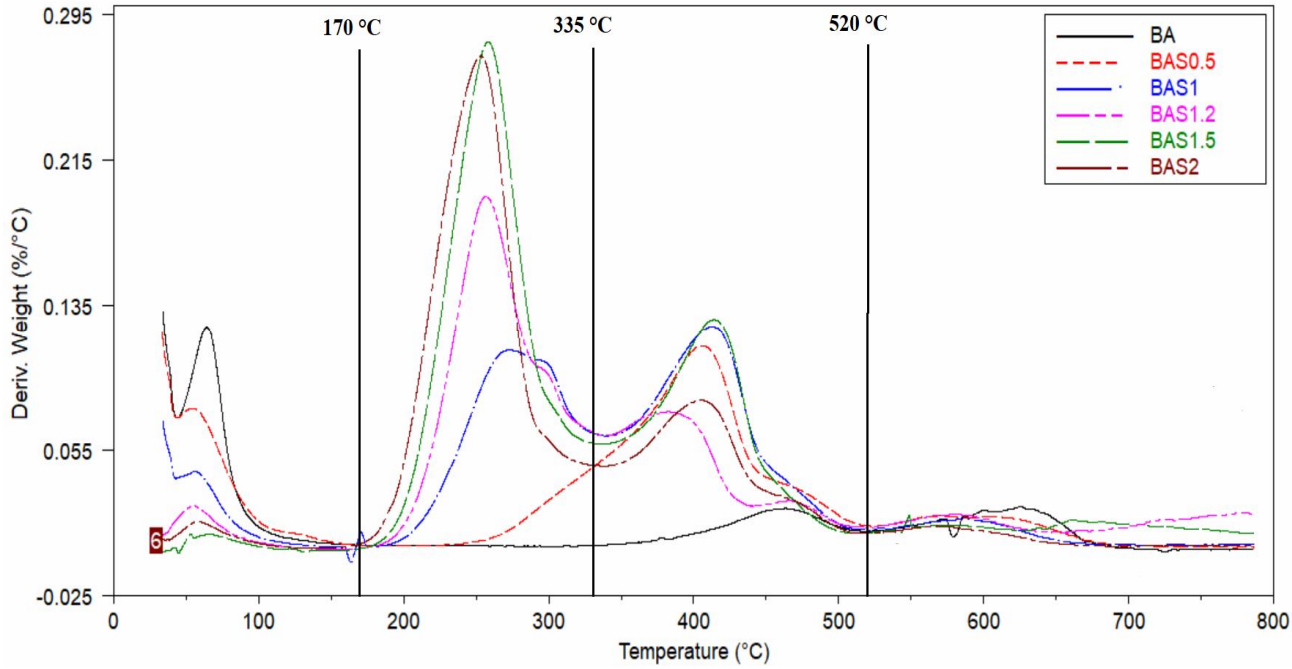

(b)

Fig. 3. TGA (a) and DTG (b) thermograms of BA and BAS samples.

Table 3. Summary of TGA Analysis of BA and BAS Samples, at Different Surfactant Concentrations

Sample	Dehydratation (water adsorbed by metal cations)	Adsorbed surfactant decomposition	Intercalated surfactant decomposition	Dehydroxylation	%Surfactant
	T < 170 ° C	170 °C < T < 335 ° C	335 °C < T < 520 ° C	T > 520 °C	
	%mass- loss	%mass- loss	%mass- loss	%mass- loss	
BA	5.31	0.41	2.3	2.55	-
BAS 0.5	4.45	2.27 - 0.41 = 1.86	10.74 - 2.3 = 8.44	2.6	10.3
BAS 1	2.26	9.8 - 0.41 = 9.39	11.88 - 2.3 = 9.58	2.2	18.97
BAS 1.2	1.05	14.25 - 0.41 = 13.84	7.98 - 2.3 = 5.68	4	19.52
BAS 1.5	0.35	18.75 - 0.41 = 18.34	11.23 - 2.3 = 8.51	1.68	26.85
BAS 2	0.78	18.68 - 0.41 = 18.27	8.3 - 2.3 = 6.0	1.62	24.27

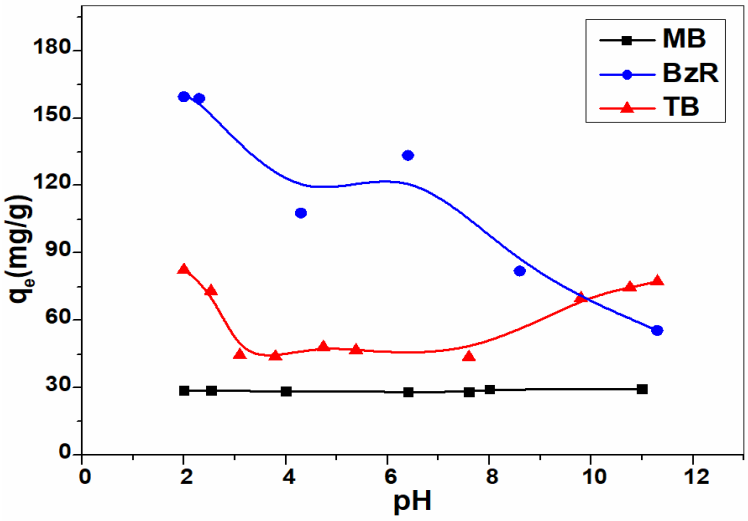

Fig. 4. Effect of pH on the adsorption of dyes onto BAS 1.5 composite.

and organophilic ones. These findings confirm the hydrophilicity loss of BAS samples [33].

The second greatest mass loss, observed within the range of 170-335 °C, turned out to be more pronounced in BAS than in BA. Since pure HDTMA bromide decomposes at about 250 °C [34], the peak observed corresponds to the decomposition of some cationic surfactant molecules adsorbed on the external surface of clay. The third most important weight loss occurred between 335 and 520 °C; it is certainly due to the decomposition of cationic surfactants

intercalated within the BA layers [35]. The last weight loss occurred between 520 and 800 °C; it corresponds to the dehydroxylation of the aluminosilicates [33].

Adsorption Studies

Effect of pH. The pH of the aqueous solution is an important parameter in the adsorption process. It is important to identify the effect of pH on adsorption, as it helps to determine the optimized operational parameters and consequently establish the most appropriate adsorption mechanism. Adsorption experiments of three different dyes onto BAS 1.5 were carried out to examine the effect of pH (in a range from 2-11) on the removal efficiency of these three dyes from an aqueous solution. The results obtained are given in Fig. 4.

It was found that the pH has no significant effect on the adsorption efficiency of methylene blue (BM). In addition, the absorption capacity at equilibrium (q_e) increased slightly (about 1 mg g^{-1}) as the pH value rose from 2 to 11.

These results are in good agreement with those described in the previous study [36]. Moreover, non-ionic dyes, like BzR, are generally water-insoluble dyes which are generally found in colloidal form [37]; they are negatively charged in solution [38]. The pH of zero point charge (pH_{PZC}) of BAS 1.5 was about 6.34 (results not shown). At pH values below and above the PZC, the organo-clay exhibited a positive and negative charge, respectively. It was found that for a pH value of about 11, the BAS 1.5 surface was less negative. Moreover, for a pH less than the PZC, BAS 1.5 composite exhibited a net positive surface charge that was attributed to the presence of ammonium groups $N^+(CH_3)_3$. For lower pH values, the removal efficiency was enhanced because of the electrostatic attraction between the negative charges of dye molecules and the positively charged surface of the adsorbent. Obviously, functional groups exhibited different degrees of ionization at different pH values. For pH values greater than the PZC, the BAS surface charge tended to be negative. When the pH value rose from 2 to 11, the adsorption of Bezathren Red (BzR) dropped. This was certainly due to the competitive adsorption between the OH^- ions and BzR dye molecules [39]. However, Telon Blue (TB) dye exhibited a different adsorption behavior.

As clearly seen in the representative curve, the adsorption capacity q_e reached two maximum values of 82.5 and 77.25 mg g^{-1}, corresponding to two pH values of 2 and 11, respectively. At pH = 2, protons were available, giving rise an increased electrostatic attraction between the negatively charged TB dye anions and the positively charged BAS 1.5 adsorption sites. The noted high adsorption capacity was certainly due to the strong electrostatic interaction between the ammonium cations of composite BAS 1.5 and the dye anions. It is important to note that the adsorption capacity decreased as the pH value augmented. Moreover, the positive charge on the composite decreased gradually and consequently the surface became negatively charged [40]. Note also that for pH values greater than 8, the adsorption capacity went up. It is worth mentioning that the surface charge of composite BAS 1.5 was less negative at pH = 11, which favored the adsorption of anionic dye molecules, probably due to hydrophobic interactions.

Effect of Contact Time

The effect of contact time on the adsorption of MB, BzR, and TB dyes, at various time points, onto the composite BAS 1.5 were investigated using a fixed adsorbent dose of 25 mg. As shown in Figure 5, the adsorption of dyes onto the organo-clay increased for longer contact time.

The result obtained is consistent with those reported in previous studies [41,42]. It is clearly noted that at the beginning, the adsorption rate of dyes was fast. After this rapid dye adsorption, the adsorbent surface became saturated and this adsorption rate dropped. The adsorption efficiency reached 80% in less than 20 min. Saturation of the BAS 1.5 composite substrate was observed at 60 min, suggesting that the aggregation of dye molecules took place around the BAS 1.5 particles. After 60 min, no significant increase in the adsorption efficiency was detected. Therefore, the contact time of 60 min was selected for all subsequent measurements.

Adsorption Kinetic Models

A kinetic study was carried out with the pseudo-first order and pseudo-second order kinetic models for the purpose of studying the adsorption process of dyes onto BAS 1.5 composite. These models are presented by Eqs.

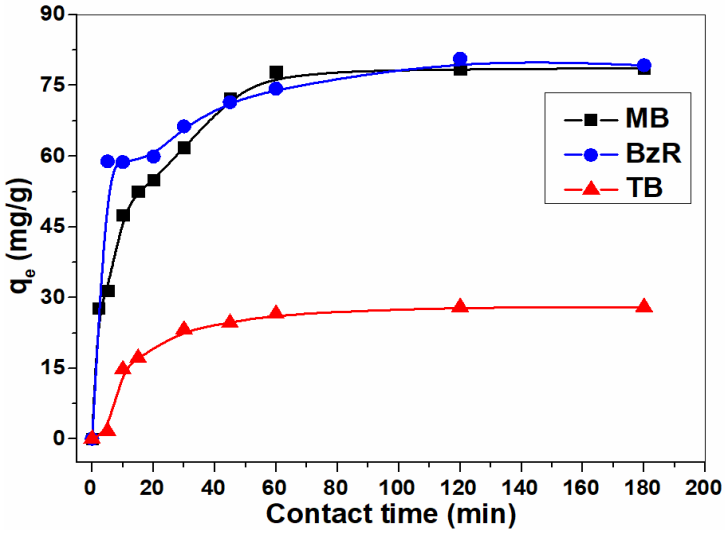

Fig. 5. Effect of time on the adsorption of dyes onto BAS 1.5 composite.

(2) and (3).

$$\ln(q_e - q_t) = \ln q_e - k_1 t \quad (2)$$

$$\frac{t}{q_t} = \frac{1}{k_2 q_e^2} + \frac{t}{q_e} \quad (3)$$

where q_e is the adsorption capacity at equilibrium (mg g^{-1}), q_t (mg g^{-1}) is the amount of dye adsorbed at time t; k_1 (min^{-1}) and k_2 (g mg^{-1} min^{-1}) are the pseudo-first and pseudo-second order rate constants, respectively.

The adsorption kinetic plots are shown in Fig. 6a and Fig. 6b. The kinetic parameters and correlation coefficient (R^2) of the two models are given in Table 4.

Regarding the pseudo-first order model, it was noted that R^2 increased from 0.781 to 0.985, and the equilibrium capacity (q_e, cal), calculated by the equation of the model, was much smaller than the experimental value (q_e, exp) for both dyes MB and TB but not for BzR. Thereby, the pseudo-first order kinetic model was not suitable to model the sorption process of MB and TB dyes onto the BAS 1.5 composite. However, the pseudo-second order kinetic model described better the adsorption processes of MB and TB based on the correlation coefficient values which were found above 0.99 and greater than those of the pseudo-first order model, except for BzR (Table 4).

Regarding the adsorption of MB and BT dyes, the suggested mechanism involved valence forces through the exchange of electrons between dye molecules and BAS 1.5 composite [43].

The adsorption mechanism of BzR which behaved as an anionic dye was probably due to the electrostatic attractions between the charged surface and charged dye molecules, considering the chemical characteristics of the surfactant-modified clay and dye molecules [44,45].

Effect of Adsorbent Dosage

The effect of the adsorbent dose on the adsorption of MB, TB and BzR dyes was studied by varying the amount of BAS 1.5 composite adsorbent. Figure 7 presents the adsorption of dyes by BAS 1.5 composite, at different adsorbent doses (10-100 mg) for the dye solution volume of 40 ml, at dye concentrations of 20, 50 and 100 mg l^{-1}, for MB, TB, and BzR, respectively.

The results presented in Fig. 7 indicate clearly that the adsorption efficiency started increasing with the adsorbent dosage at the beginning, suggesting that a greater surface area and more adsorption sites are available. The optimal BAS composite adsorbent dose for the adsorption of TB and BzR dyes was found to be 40 mg; however, a better dose (25 mg) was needed for the adsorption of MB. Moreover, for m > 25 mg, no significant variation in the adsorption

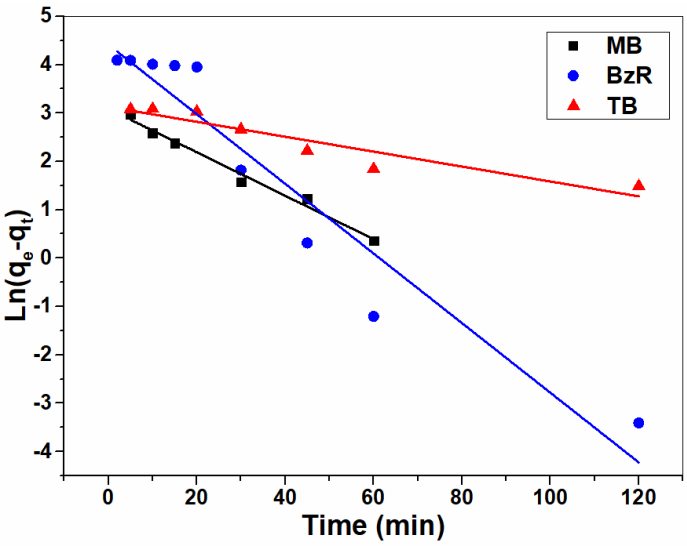

(a)

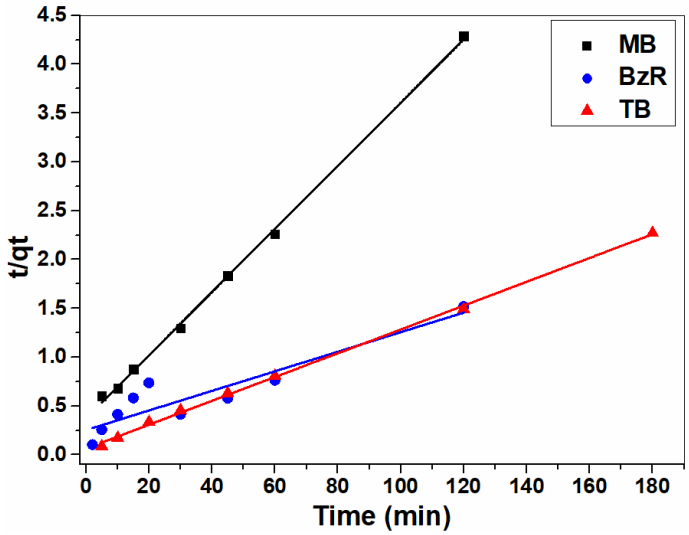

(b)

Fig. 6. a) Pseudo-first-order kinetics model (a) and pseudo-second-order kinetics model (b) for the adsorption of different dyes on BAS 1.5 composite.

efficiency was observed for MB. Therefore, the dose of 25 mg of BAS 1.5 composite was selected for all subsequent measurements.

Adsorption Isotherm Studies

The adsorption isotherms were studied by mixing 25 mg of the composite with a series of MB, TB, and BzR solutions, at different initial concentrations (from 5 to 200 mg l^{-1}); the mixtures thus obtained were stirred for 60 min. Figure 8 indicates that at low equilibrium concentrations, the adsorption capacities increased quickly. Note that the values of q_e increased slowly when C_e was

Table 4. Pseudo-first and Pseudo-second Order Kinetic Parameters for the Adsorption of Dyes onto BAS 1.5 Composite

Dye	q_e (exp) (mg g^{-1})	Pseudo-first order			Pseudo-second order		
		k_1 (min^{-1})	q_e (cal) (mg g^{-1})	R^2	k_2 (min^{-1})	q_e (cal) (mg g^{-1})	R^2
BM	28	0.044	21.86	0.985	0.0034	31.25	0.998
BzR	79.73	0.072	82.59	0.923	0.00039	100	0.852
TB	80.64	542	5.002	0.781	0.2	100	0.999

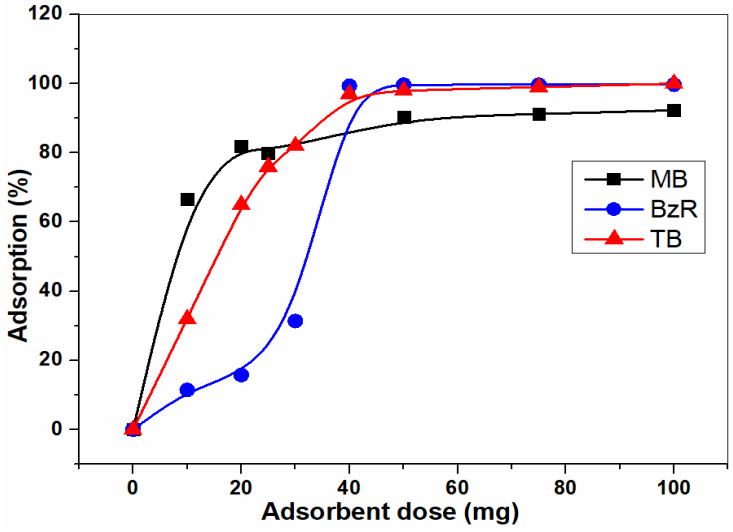

Fig. 7. Effect of adsorbent dose on the adsorption of dyes onto BAS 1.5 composite.

within the range [10-20 mg l^{-1}] for adsorption of all dyes. However, when C_e increased beyond 100 mg l^{-1}, the q_e values remained nearly unchanged. These findings suggest that the initial dye concentration is an important parameter in the adsorption process.

Langmuir and Freundlich isotherms are presented by Eqs. (4) and (5):

$$\frac{C_e}{q_e} = \frac{C_e}{q_{\max}} + \frac{1}{q_{\max} . K_L} \quad (4)$$

$$\ln q_e = \ln K_F + \frac{1}{n} \ln C_e \quad (5)$$

where C_e is the equilibrium concentration of dye (mg l^{-1}), q_e is the amount of dye adsorbed on BAS 1.5 composite (mg g^{-1}), K_L is the Langmuir adsorption constant (l mg^{-1}), q_{max} is the maximum monolayer adsorption capacity of the adsorbent (mg g^{-1}), K_F is the Freundlich adsorption constant, which is related to the adsorption capacity, and n is the heterogeneity factor. The Langmuir and Freundlich

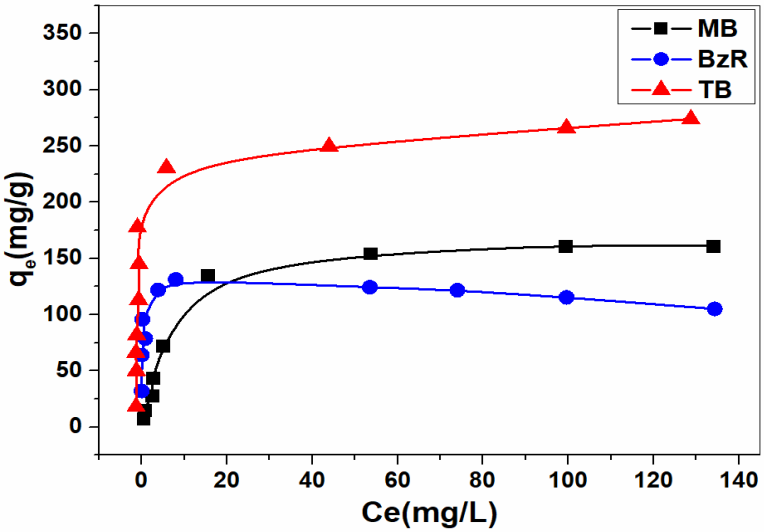

Fig. 8. Effect of initial dye concentration on the adsorption of dyes onto BAS 1.5 composite

Table 5. Langmuir and Freundlich Isotherm Parameters for the Adsorption of MB, TB and BzR Dyes *onto* BAS1.5 Ccomposite

Dye	pH	Langmuir			Freundlich		
		K_L (l mg^{-1})	q_m (mg g^{-1})	R^2	K_F (l g^{-1})	1/n	R^2
MB	6.4	0.139	166.67	0.997	20.106	0.542	0.895
TB	11	0.125	500	0.971	116.62	0.210	0.537
BzR	2.5	225.00	111.11	0.994	89.57	0.103	0.614

adsorption isotherms for dyes adsorbed onto BAS 1.5 composite are presented in Fig. 9. The isotherm parameters obtained from these models are summarized in Table 5. The equilibrium data were fit better to the Langmuir model than to the Freundlich model, as can be seen in Fig. 9. This is indicative of the homogeneity of the adsorption sites on the BAS 1.5 composite particles. In addition, as clearly indicated in Table 5, all 1/n values are below 1, indicating a normal Langmuir isotherm. However, the 1/n value above unity is indicative of the cooperative adsorption [46], and the values of 1/n between 0.103 and 0.542 are indicative of a favorable adsorption [47].

Thermodynamic Studies

The influence of temperature on the adsorption behavior of different dyes onto BAS 1.5 composite was also investigated under optimized conditions, at the temperatures of 298, 303, 313 and 323 K. A thermodynamic analysis was conducted to understand the characteristics and mechanisms of adsorption. The thermodynamic parameters ΔG°, ΔH°,

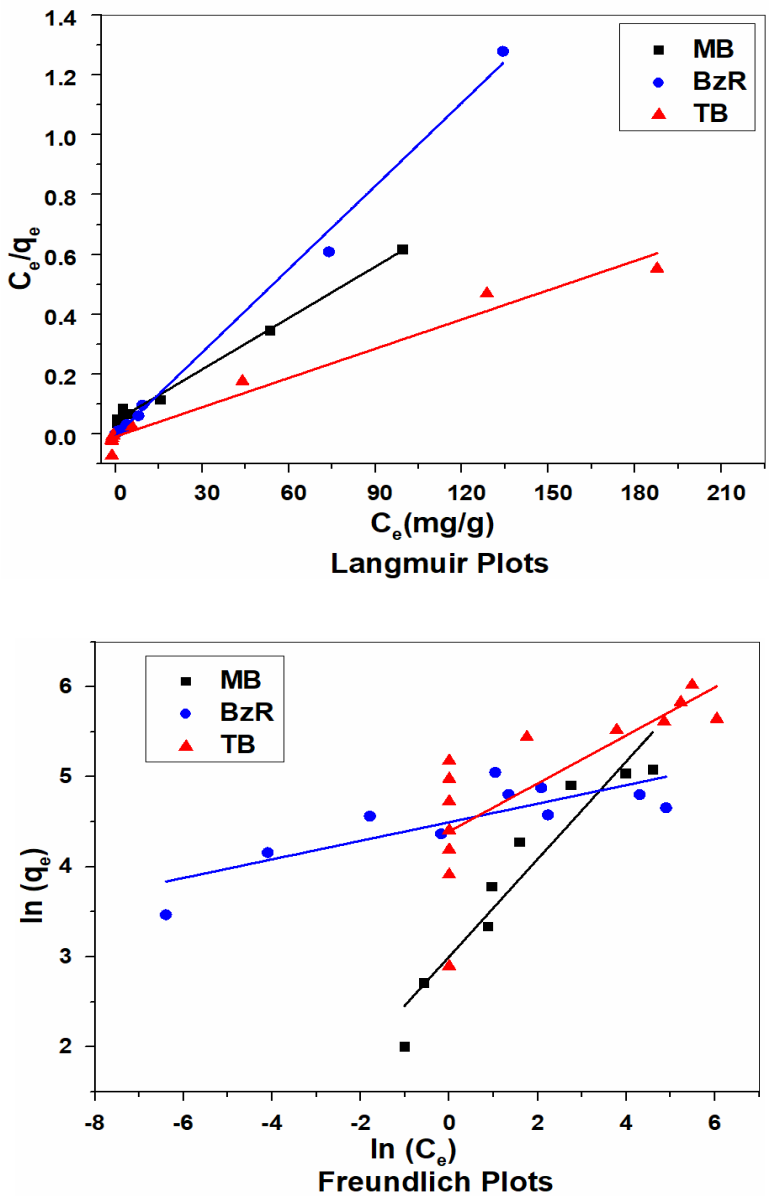

Fig. 9. Isotherm plots for the adsorption of dyes onto BAS1.5.

and ΔS° were calculated using Eqs. (6), (7) and (8).

$$K_d = q_e/C_e \quad (6)$$

$$\Delta G^\circ = -RT\ln K_d \quad (7)$$

$$\ln K_d = \frac{\Delta S^\circ}{R} - \frac{\Delta H^\circ}{RT} \quad (8)$$

where K_d is the distribution coefficient (l g^{-1}), T is the temperature (K), and R is the gas constant (8.314 J mol^{-1} K^{-1}). The enthalpy change (ΔH° (kJ mol^{-1})) and the entropy change (ΔS° (J mol^{-1} K^{-1}) were computed from the slope and intercept of the linear plot of $\ln K_d$ *vs.* 1/T, as presented in Fig. 10.

The previously calculated thermodynamic parameters ΔG°, ΔH° and ΔS° are summarized in Table 6. Generally,

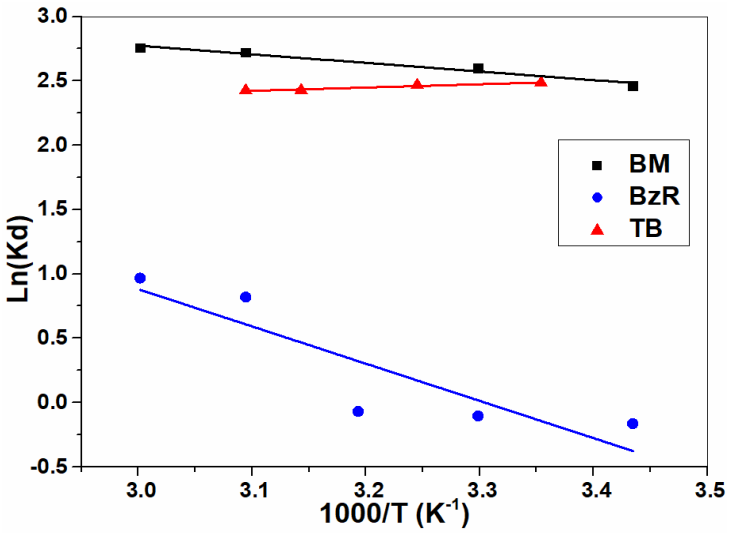

Fig. 10. The Van't Hoff plots for the adsorption of dyes onto BAS1.5 composite.

Table 6. Thermodynamic Parameters for the Adsorption Process of dyes onto BAS1.5 Composite at Various Temperatures

Dye	ΔH° (kJ mol^{-1})	ΔS° (J mol^{-1} K^{-1})	ΔG° (kJ mol^{-1})			
			298 K	303 K	313 K	323 K
MB	12.11	58.6	-5.36	-5.65	-6.24	-6.83
TB	2.09	13.64	-1.98	-2.04	-2.18	-2.32
BzR	24.04	79.46	0.36	-0.048	-0.84	-1.64

the absolute magnitude of free energy change for physisorption is between -20 and 0 kJ mol^{-1} [48].

The results concerning the adsorption process of BM, BT and BzR dyes, at 298, 303, 313, 323 K, show that the free energy values were negative, indicating a spontaneous and favorable adsorption process onto BAS 1.5 composite, except for BzR at 298 K. The positive ΔG° value suggests that the adsorption is non-spontaneous and less favorable at that temperature. It is worth recalling that positive values of ΔH° imply an endothermic reaction. The positive values of ΔS° indicate an increase in entropy and the solid-liquid interface becomes more random during the adsorption process of dyes.

In conclusion, the adsorption capacity of BM, BzR and TB dyes at 298 K obtained in this study is compared with those determined by other authors [48-51]. These results are given in Table 7.

Proposed Adsorption Mechanism

The composite under study consists of bentonite clay and surfactant. According to the literature [52,53], and based on the composite structure, the hydrophilic adsorption occurs between the composite and different dyes, as shown in Fig. 11. It is worth mentioning that the quaternary ammonium cationic surfactant turns the composite hydrophilic. It is widely acknowledged that cationic

Table 7. Comparison of the Mmaximum Adsorption Capacities for BM, BzR and TB Adsorption on BAS 1.5 with Those of other Adsorbents

Dye	Adsorbent	Maximum adsorption capacity ($mg\ g^{-1}$)	Ref.
MB	Montmorillonite	74	[48]
	Acid modified clay beads	223.19	[49]
	BAS 1.5	166.67	Present study
TB	Mesoporous silicate/polypyrrole	55.55	[50]
	BAS 1.5	500	Present study
BzR	Sodic Montmorillonite	48.52	[51]
	BAS 1.5	111.11	Present study

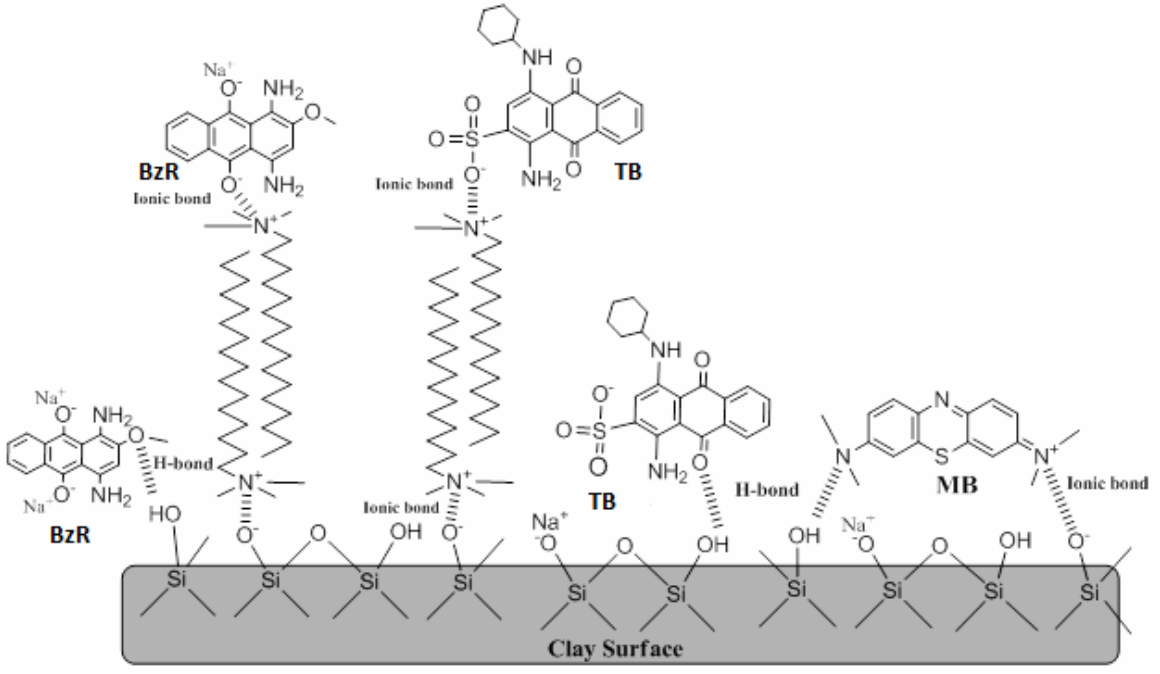

Fig. 11. Proposed mechanism for the adsorption of Telon Blue, Bezathren Red and Methylene Blue onto BAS1.5 composite.

surfactants can produce strong electrostatic adsorption of anionic dyes. This process leads to ultrahigh adsorption capacities of the composite for BzR and TB molecules. Moreover, hydrogen bonding may occur between the oxygen silanol groups of bentonite and both of nitrogen and oxygen atoms of dyes. Therefore, the excellent adsorption

properties of BAS composite can be attributed to the synergistic effect of hydrogen bonding and the electrostatic interactions between the adsorbent and MB, TB and BzR dyes.

CONCLUSIONS

In this study, the BAS composite was prepared by the modification of bentonite with the HDTMA surfactant loadings from 50 to 200% of CEC. The resulting composites were characterized by X-ray diffraction (XRD), infrared spectroscopy (FTIR) and thermal analysis (ATG/DTG).

The adsorption of Methylene Blue (MB), Bezathren Red (BzR), and Telon Blue (TB) dyes onto BAS 1.5 composite were studied using batch tests conducted under different experimental conditions, while the parameters such as the contact time, pH of dye solution, adsorbent dosage, initial dye concentrations, and temperature changed. The kinetic study showed that the adsorption process of all dyes can be described by the pseudo-second order model.

The equilibrium data were analyzed using the Langmuir and Freundlich models, but the first one was found more appropriate for describing the adsorption of MB, BzR and TB dyes. In addition, the calculated Langmuir maximum adsorption capacities of MB, BzR, and TB were found equal to 166.67, 111.11 and 500 mg g^{-1}, respectively, and the adsorption process turned out to be endothermic in nature in all cases (MB, TB and BzR). The adsorption capacities of BM, BzR, and TB dyes at 298 K, obtained in this study, were found to be more effective than those reported by other authors in the literature. These findings allow stating that BAS composite can be employed as a low-cost material for the removal of cationic, anionic and vat dyes from effluents.

REFERENCES

[1] De Jesus da Silveira Neta, J.; Costa Moreira, G.; da Silva, C. J.; Reis, C.; Reis, E. L., Use of polyurethane foams for the removal of the direct red 80 and reactive blue 21 dyes in aqueous medium. *Desalination* **2011**, *281*, 55-60, DOI: 10.1016/j.desal.2011.07.041.

[2] Kono, H., Preparation and characterization of amphoteric cellulose hydrogels as adsorbents for the anionic dyes in aqueous solutions. *Gels* **2015**, *1*, 94-116, DOI: 10.3390/gels1010094.

[3] Ngulube, T.; Gumbo, J. R.; Masindi, V.; Maity, A., An update on synthetic dyes adsorption onto clay based minerals: A state-of-art review. *J. Environ. Manage.* **2017**, *191*, 35-57, DOI: 10.1016/j.jenvman.2016.12.031.

[4] Kuppusamy, S.; Thavamani, P.; Megharaj, M.; Venkateswarlu, K.; Lee, Y. B.; Naidu, R., Potential of melaleuca diosmifolia as a novel, non-conventional and low-cost coagulating adsorbent for removing both cationic and anionic dyes. *J. Ind. Eng. Chem.* **2016**, *37*, 198-207, DOI: 10.1016/j.jiec.2016.03.021.

[5] Çelekli, A.; Birecikligil, S. S.; Geyik, F.; Bozkurt, H., Prediction of removal efficiency of lanaset red G on walnut husk using artificial neural network model. *Bioresour. Technol.* **2012**, *103*, 64-70, DOI: 10.1016/j.biortech.2011.09.106.

[6] Zhu, H. Y.; Jiang, R.; Fu, Y. Q.; Jiang, J. H.; Xiao, L.; Zeng, G. M., Preparation, characterization and dye adsorption properties of γ-Fe_2O_3/SiO_2/Chitosan Composite. Appl. Surf. Sci. 2011, 258, 1337-1344, DOI: 10.1016/j.apsusc.2011.09.045.

[7] Xu, R. Kou; Xiao, S. Cheng; Yuan, J. Hua; Zhao, A. Zhen., Adsorption of methyl violet from aqueous solutions by the biochars derived from crop residues. *Bioresour. Technol.* **2011**, *102*, 10293-10298, DOI: 10.1016/j.biortech.2011.08.089.

[8] Akgül, M.; Karabakan, A., Promoted dye adsorption performance over desilicated natural zeolite. *Microporous Mesoporous Mater.* **2011**, *145*, 157-164, DOI: 10.1016/j.micromeso.2011.05.012.

[9] Huang, X. Y.; Bu, H. T.; Jiang, G. B.; Zeng, M. H., Cross-linked succinyl chitosan as an adsorbent for the removal of methylene blue from aqueous solution. *Int. J. Biol. Macromol.* **2011**, *49*, 643-651, DOI: 10.1016/j.ijbiomac.2011.06.023.

[10] Heddi, D.; Benkhaled, A.; Boussaid, A.; Choukchou-Braham, E., Adsorption of anionic dyes on poly(N-vinylpyrrolidone) modified bentonite. *Phys. Chem. Res.* **2019**, *7*, 731-749, DOI: 10.22036/pcr.2019.179510.1625.

[11] Medjahed, K.; Tennouga, L.; Mansri, A.; Chetouani,

A.; Hammouti, B.; Desbrières, J., Interaction between poly(4-vinylpyridine-graft-bromodecane) and textile blue basic dye by spectrophotometric study. *Res. Chem. Intermed.* **2013**, *39*, 3199-3208, DOI: 10.1007/s11164-012-0832-2.

[12] Ghaedi, M.; Hossainian, H.; Montazerozohori, M.; Shokrollahi, A.; Shojaipour, F.; Soylak, M.; Purkait, M. K., A Novel Acorn Based Adsorbent for the Removal of Brilliant Green. *Desalination* **2011**, *281*, 226-233, DOI: 10.1016/j.desal.2011.07.068.

[13] Elmoubarki, R.; Mahjoubi, F. Z.; Tounsadi, H.; Moustadraf, J.; Abdennouri, M.; Zouhri, A.; El Albani, A.; Barka, N., Adsorption of textile dyes on raw and decanted moroccan clays: Kinetics, equilibrium and thermodynamics. *Water Resour. Ind.* **2015**, *9*, 16-29, DOI: 10.1016/j.wri.2014.11.001.

[14] Bouberka, Z.; Khenifi, A.; Benderdouche, N.; Derriche, Z., Removal of supranol yellow 4GL by adsorption onto Cr-intercalated montmorillonite. *J. Hazard. Mater.* **2006**, *133*, 154-161, DOI: 10.1016/j.jhazmat.2005.10.003.

[15] Mousavi, S. M.; Babapoor, A.; Hashemi, S. A.; Medi, B. C. Adsorption and removal characterization of nitrobenzene by graphene oxide coated by polythiophene nanoparticles. *Phys. Chem. Res.* **2020**, *8*, 225-240, DOI: 10.22036/pcr.2020.208780.1700.

[16] Ait Himi, M.; El Ghachtouli, S.; Amarray, A.; Zaroual, Z.; Bonnaillie, P.; Azzi, M., Removal of azo dye calcon using polyaniline films electrodeposited on SnO_2 substrate. *Phys. Chem. Res.* **2020**, *8*, 111-124, DOI: 10.22036/pcr.2019.203023.1680.

[17] Salari, H.; Kohantorabi, M., Fabrication of novel $Fe_2O_3/MoO_3/AgBr$ nanocomposites with enhanced photocatalytic activity under visible light irradiation for organic pollutant degradation. *Adv. Powder Technol.* **2020**, *31*, 493-503, DOI: 10.1016/j.apt.2019.11.005.

[18] Salari, H.; Kohantorabi, M., Facile template-free synthesis of new α-MnO_2 nanorod/silver iodide p-n junction nanocomposites with high photocatalytic performance. *New J. Chem.* **2020**, *44*, 7401-7411, DOI: 10.1039/d0nj01033b.

[19] Ali, I.; Asim, M.; Khan, T. A., Low cost adsorbents for the removal of organic pollutants from wastewater. *J. Environ. Manage.* **2012**, *113*, 170-183, DOI: 10.1016/j.jenvman.2012.08.028.

[20] Özcan, A. S.; Erdem, B.; Özcan, A., Adsorption of acid blue 193 from aqueous solutions onto Na-bentonite and DTMA-bentonite. *J. Colloid Interface Sci.* **2004**, *280*, 44-54, DOI: 10.1016/j.jcis.2004.07.035.

[21] Kaya, E. M. Ö.; Özcan, A. S.; Gök, Ö.; Özcan, A., Adsorption kinetics and isotherm parameters of naphthalene onto natural- and chemically modified bentonite from aqueous solutions. *Adsorption* **2013**, *19*, 879-888, DOI: 10.1007/s10450-013-9542-3.

[22] Wang, L.; Wang, A., Adsorption properties of congo red from aqueous solution onto surfactant-modified montmorillonite. *J. Hazard. Mater.* **2008**, *160*, 173-180, DOI: 10.1016/j.jhazmat.2008.02.104.

[23] Açışlı, Ö.; Karaca, S.; Gürses, A., Investigation of the alkyl chain lengths of surfactants on their adsorption by montmorillonite (Mt) from aqueous solutions. *Appl. Clay Sci.* **2017**, *142*, 90-99, DOI: 10.1016/j.clay.2016.12.009.

[24] Yang, S.; Gao, M.; Luo, Z., Adsorption of 2-naphthol on the organo-montmorillonites modified by gemini surfactants with different spacers. *Chem. Eng. J.* **2014**, *256*, 39-50, DOI: 10.1016/j.cej.2014.07.004.

[25] Makhoukhi, B.; Djab, M.; Amine Didi, M., Adsorption of telon dyes onto bis-imidazolium modified bentonite in aqueous solutions. *J. Environ. Chem. Eng.* **2015**, *3*, 1384-1392, DOI: 10.1016/j.jece.2014.12.012.

[26] Monvisade, P.; Siriphannon, P., Chitosan intercalated montmorillonite: Preparation, characterization and cationic dye adsorption. *Appl. Clay Sci.* **2009**, *42*, 427-431, DOI: 10.1016/j.clay.2008.04.013.

[27] Huang, P.; Kazlauciunas, A.; Menzel, R.; Lin, L., Determining the mechanism and efficiency of industrial dye adsorption through facile structural control of organo-montmorillonite adsorbents. ACS *Appl. Mater. Interfaces* **2017**, *9*, 26383-26391, DOI: 10.1021/acsami.7b08406.

[28] Darder, M.; Colilla, M.; Ruiz-Hitzky, E., Biopolymer-clay nanocomposites based on chitosan intercalated in montmorillonite. *Chem. Mater.* **2003**, *15*, 3774-3780, DOI: 10.1021/cm0343047.

[29] Parolo, M. E.; Pettinari, G. R.; Musso, T. B.; Sánchez-Izquierdo, M. P.; Fernández, L. G., Characterization of organo-modified bentonite sorbents: The effect of modification conditions on adsorption performance. *Appl. Surf. Sci.* **2014**, *320*, 356-363, DOI: 10.1016/j.apsusc.2014.09.105.

[30] Vaia, R. A.; Teukolsky, R. K.; Giannelis, E. P., Interlayer structure and molecular environment of alkylammonium layered silicates. *Chem. Mater.* **1994**, *6*, 1017-1022, DOI: 10.1021/cm00043a025.

[31] Xie, W.; Gao, Z.; Pan, W. P.; Hunter, D.; Singh, A.; Vaia, R., Thermal degradation chemistry of alkyl quaternary ammonium montmorillonite. *Chem. Mater.* **2001**, *13*, 2979-2990, DOI: 10.1021/cm010305s.

[32] Zhu, J.; Morgan, A. B.; Lamelas, F. J.; Wilkie, C. A., Fire properties of polystyrene-clay nanocomposites. *Chem. Mater.* **2001**, *13*, 3774-3780, DOI: 10.1021/cm000984r.

[33] Xi, Y.; Mallavarapu, M.; Naidu, R., Preparation, characterization of surfactants modified clay minerals and nitrate adsorption. *Appl. Clay Sci.* **2010**, *48*, 92-96, DOI: 10.1016/j.clay.2009.11.047.

[34] Erdem, B.; Özcan, A. S.; Özcan, A., Preparation of HDTMA-bentonite: Characterization studies and its adsorption behavior toward dibenzofuran. *Surf. Interface Anal.* **2010**, *42*, 1351-1356, DOI: 10.1002/sia.3230.

[35] Majdan, M.; Pikus, S.; Gajowiak, A.; Sternik, D.; Zieba, E., Uranium sorption on bentonite modified by octadecyltrimethylammonium bromide. *J. Hazard. Mater.* **2010**, *184*, 662-670, DOI: 10.1016/j.jhazmat.2010.08.089.

[36] Jourvand, M.; Shams Khorramabadi, G.; Omidi Khaniabadi, Y.; Godini, H.; Nourmoradi, H., Removal of methylene blue from aqueous solutions using modified clay. *J. Basic Res. Med. Sci.* **2015**, *2*, 32-41.

[37] Gupta, V. K.; Suhas, Application of low-cost adsorbents for dye removal-A review. *J. Environ. Manage.* **2009**, *90*, 2313-2342, DOI: 10.1016/j.jenvman.2008.11.017.

[38] Kim, T. H.; Park, C.; Shin, E. B.; Kim, S., Decolorization of disperse and reactive dye solutions using ferric chloride. *Desalination* **2004**, *161*, 49-58, DOI: 10.1016/S0011-9164(04)90039-2.

[39] Binaeian, E.; Seghatoleslami, N.; Chaichi, M. J., Synthesis of oak gall tannin-immobilized hexagonal mesoporous silicate (OGT-HMS) as a new super adsorbent for the removal of anionic dye from aqueous solution. *Desalin. Water Treat.* **2016**, *57*, 8420-8436, DOI: 10.1080/19443994.2015.1020513.

[40] Zohra, B.; Aicha, K.; Fatima, S.; Nourredine, B.; Zoubir, D., Adsorption of Direct Red 2 on Bentonite Modified by Cetyltrimethylammonium Bromide. *Chem. Eng. J.* **2008**, *136*, 295-305, DOI: 10.1016/j.cej.2007.03.086.

[41] Rajabi, M.; Mirza, B.; Mahanpoor, K.; Mirjalili, M.; Najafi, F.; Moradi, O.; Sadegh, H.; Shahryari-ghoshekandi, R.; Asif, M.; Tyagi, I.; Agarwal, S.; Gupta, V. K., Adsorption of Malachite Green from Aqueous Solution by Carboxylate Group Functionalized Multi-Walled Carbon Nanotubes: Determination of Equilibrium and Kinetics Parameters. *J. Ind. Eng. Chem.* **2016**, *34*, 130-138, DOI: 10.1016/j.jiec.2015.11.001.

[42] Bhatt, A. S.; Sakaria, P. L.; Vasudevan, M.; Pawar, R. R.; Sudheesh, N.; Bajaj, H. C.; Mody, H. M., Adsorption of an Anionic Dye from Aqueous Medium by Organoclays: Equilibrium Modeling, Kinetic and Thermodynamic Exploration. *RSC Adv.* **2012**, *2*, 8663-8671, DOI: 10.1039/c2ra20347b.

[43] Orucoglu, E.; Haciyakupoglu, S., Bentonite modification with hexadecylpyridinium and aluminum polyoxy cations and its effectiveness in Se(IV) removal. *J. Environ. Manage.* **2015**, *160*, 30-38, DOI: 10.1016/j.jenvman.2015.06.005.

[44] Keyhanian, F.; Shariati, S.; Faraji, M.; Hesabi, M., Magnetite nanoparticles with surface modification for removal of methyl violet from aqueous solutions. *Arab. J. Chem.* **2016**, *9*, S348-S354, DOI: 10.1016/j.arabjc.2011.04.012.

[45] Muthukumaran, C.; Sivakumar, V. M.; Thirumarimurugan, M., Adsorption isotherms and kinetic studies of crystal violet dye removal from aqueous solution using surfactant modified magnetic nanoadsorbent. *J. Taiwan Inst. Chem. Eng.* **2016**, *63*, 354-362, DOI: 10.1016/j.jtice.2016.03.034.

[46] Jović-Jovičić, N.; Milutinović-Nikolić, A.; Gržetic, I.; Jovanović, D., Organobentonite as efficient textile dye

sorbent. *Chem. Eng. Technol.* **2008**, *31*, 567-574, DOI: 10.1002/ceat.200700421.

[47] Hameed, B. H.; Din, A. T. M.; Ahmad, A. L., Adsorption of methylene blue onto bamboo-based activated carbon: Kinetics and equilibrium studies. *J. Hazard. Mater.* **2007**, *141*, 819-825, DOI: 10.1016/j.jhazmat.2006.07.049.

[48] Yu, Y.; Zhuang, Y. Y.; Wang, Z. H., Adsorption of water-soluble dye onto functionalized resin. *J. Colloid Interface Sci.* **2001**, *242*, 288-293, DOI: 10.1006/jcis.2001.7780.

[49] Zhou, K.; Zhang, Q.; Wang, B.; Liu, J.; Wen, P.; Gui, Z.; Hu, Y., The integrated utilization of typical clays in removal of organic dyes and polymer nanocomposites. *J. Clean. Prod.* **2014**, *81*, 281-289, DOI: 10.1016/j.jclepro.2014.06.038.

[50] Auta, M.; Hameed, B. H., Acid modified local clay beads as effective low-cost adsorbent for dynamic adsorption of methylene blue. *J. Ind. Eng. Chem.* **2013**, *19*, 1153-1161, DOI: 10.1016/j.jiec.2012.12.012.

[51] Belbachir, I.; Makhoukhi, B., Adsorption of bezathren dyes onto sodic bentonite from aqueous solutions. *J. Taiwan Inst. Chem. Eng.* **2017**, *75*, 105-111, DOI: 10.1016/j.jtice.2016.09.042.

[52] Errais, E.; Duplay, J.; Elhabiri, M.; Khodja, M.; Ocampo, R.; Baltenweck-Guyot, R.; Darragi, F., Anionic RR120 dye adsorption onto raw clay: Surface properties and adsorption mechanism. *Colloids Surfaces A Physicochem. Eng. Asp.* **2012**, *403*, 69-78, DOI: 10.1016/j.colsurfa.2012.03.057.

[53] Mahmoodi, N. M.; Abdi, J.; Taghizadeh, M.; Taghizadeh, A.; Hayati, B.; Shekarchi, A. A.; Vossoughi, M., Activated carbon/metal-organic framework nanocomposite: Preparation and photocatalytic dye degradation mathematical modeling from wastewater by least squares support vector machine. *J. Environ. Manage.* **2019**, *233*, 660-672, DOI: 10.1016/j.jenvman.2018.12.026.